

Dirac semimetal PdTe₂ temperature-dependent quasiparticle dynamics and electron-phonon coupling

Shu-Yu Liu,¹ Shuang-Xing Zhu,¹ Qi-Yi Wu,¹ Chen Zhang,¹ Peng-Bo Song,^{2,3} You-Guo Shi,^{2,3} Hao Liu,¹ Zi-Teng Liu,¹ Jiao-Jiao Song,¹ Fan-Ying Wu,¹ Yin-Zou Zhao,¹ Xiao-Fang Tang,¹ Ya-Hua Yuan,¹ Han Huang,¹ Jun He,¹ H. Y. Liu,⁴ Yu-Xia Duan,¹ and Jian-Qiao Meng^{1,5,*}

¹*School of Physics and Electronics, Central South University, Changsha 410083, Hunan, China*

²*Beijing National Laboratory for Condensed Matter Physics,*

Institute of Physics, Chinese Academy of Sciences, Beijing 100190, China

³*School of Physical Sciences, University of Chinese Academy of Sciences, Beijing 100049, China*

⁴*Beijing Academy of Quantum Information Sciences, Beijing 100085, China*

⁵*Synergetic Innovation Center for Quantum Effects and Applications (SICQEA),*

Hunan Normal University, Changsha 410081, China

(Dated: Saturday 5th March, 2022)

Dirac semimetal PdTe₂ single-crystal temperature-dependent ultrafast carrier and phonon dynamics were studied using ultrafast optical pump-probe spectroscopy. Two distinct carrier and coherent phonons relaxation processes were identified in the 5 K - 300 K range. Quantitative analysis revealed a fast relaxation process (τ_f) occurring on a subpicosecond time scale which originated from electron-phonon thermalization. This was followed by a slower relaxation process (τ_s) with a time scale of ~ 7 -9.5 ps which originated from phonon-assisted electron-hole recombination. Two significant vibrational modes resolved at all measured temperatures and corresponded to Te atoms in-plane (E_g), and out-of-plane (A_{1g}), motion. As temperature increased both phonon modes softened markedly. A_{1g} mode frequency monotonically decreased as temperature increased. Its damping rate remained virtually unchanged. As expected, E_g decreased uniformly as temperatures rose. At temperatures above 80 K, there was insignificant change. Test results suggested that pure dephasing played an important role in the relaxation processes. PdTe₂ phonon is thought responsible for its superconductive properties. Examining phonons behavior should improve the understanding of its complex superconductivity.

PACS numbers: 74.25.Jb,71.18.+y,74.72.-h,79.60.-i

I. INTRODUCTION

Recently, layered, transition-metal dichalcogenides (TMDCs) have been extensively studied for their electronic properties and photoelectric qualities in such fields as superconductivity, nontrivial topological properties, charge density waves, extremely large positive magnetoresistance, and others [1–5]. After topological insulators were discovered [6, 7], topological superconductors attracted extensive research interest [8, 9]. It was expected that by tuning the topological superconductivity state, such as by tuning Majorana fermions, a new quantum computation class could be realized. For TMDCs, several different physical properties coexist simultaneously [10, 11]. Theoretical calculations and experimental results suggest several TMDC materials may have topological superconductivity [12–16].

PdTe₂ is favored for its outstanding physical properties. Its superconductivity, with superconducting transition temperatures $T_c \sim 1.7$ K, was discovered in the 1960s [17]. Point-contact spectroscopy, heat capacity, tunneling, and other tests suggested that PdTe₂ is a fully-gapped, s -wave conventional superconductor. The bulk is a typical type-I superconductor. Its surface is a mix of type-I and type-II superconductivity [13, 18–23]. Recently, angle-resolved photoemission spectroscopy

(ARPES) confirmed that PdTe₂ is either a type-II, or a type-I and type-II co-existent, Dirac semimetal with a spin-polarized topological surface state [24–28]. PdTe₂ was considered as a candidate to realize topological superconductivity [13, 14]. Prior Neutron inelastic scattering [29] and recent theoretical calculations [30] suggest that a dip structure in the phonon dispersion near Γ is important for PdTe₂ superconductivity. It holds great promise to study the temperature dependence of the phonons in PdTe₂ with an eye towards their importance for superconductivity.

Ultrafast optical pump-probe spectroscopy is a powerful tool for studying quasiparticle dynamics especially the temperature evolution behaviors of low energy scale collective modes. These are usually far beyond ARPES energy resolution limits [31–35]. ARPES, also a powerful tool for detecting the many-body effects has yet to identify PdTe₂ phonons [24–28, 36]. Ultrafast optical pump-probe spectroscopy was very suitable for studying this issue.

Detailed, temperature-dependent, ultrafast optical pump-probe spectroscopy measurements were performed to investigate excited collective mode dynamics in single PdTe₂ crystals. Two distinct carrier relaxation process with different time scales were observed. They originated from from electron-phonon (e - ph) thermalization

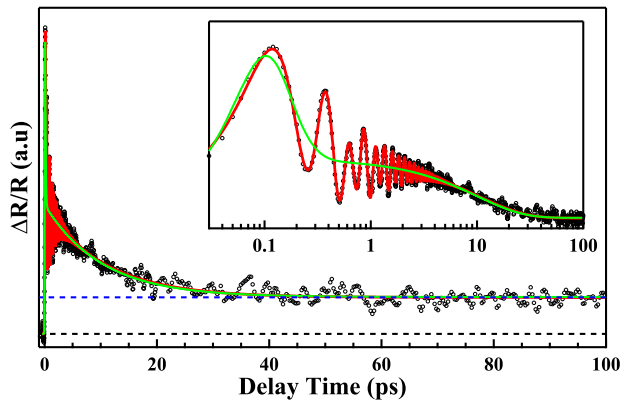


FIG. 1. (Color online) $\Delta R/R$ transient reflectivity is shown as a function of delay time in PdTe₂ at 100 K up to 100 ps. The solid red line, oscillation present, and solid green line, oscillation absent, show measured signal fit. The dashed blue line indicated $\Delta R/R$ value at long delays.

(τ_f) and phonon-assisted electron-hole ($e-h$) recombination (τ_s), respectively. Two optical phonons, in-plane (E_g), and out-of-plane (A_{1g}) Te atoms motions, were extracted at temperatures ranging from 5 K - 300 K. E_g energy was consistent with that of a Γ phonon which is thought to be responsible for PdTe₂ superconductivity [29, 30].

II. EXPERIMENT

Ultrafast time-resolved differential reflectivity $\Delta R/R$ was performed on a high-quality PdTe₂ single crystal with a pulse laser produced by a Ti: sapphire femtosecond (fs) laser oscillator. Pulses width was ~ 35 fs with a center wavelength of 800 nm (1.55 eV) and a repetition rate of 1 MHz. Pump and probe pulses were focused on the sample at nearly normal incidence with spot size diameter of $\simeq 160$ and $40 \mu\text{m}$, respectively. Pump fluence was $F = 25 \mu\text{J}/\text{cm}^2$. The pump-probe was cross-polarized. Data was collected on a freshly cleaved surface from 5 K - 300 K. All measurements were carried out under high vacuum (10^{-6} mbar). The flux method was used to grow high quality PdTe₂ single crystals [22].

III. RESULTS AND DISCUSSION

PdTe₂ differential reflectivity $\Delta R/R$ at $T = 100$ K in linear (main panel) and log (inset) timescales is shown in Fig. 1. Electron-electron ($e-e$) thermalization and electron-boson scattering processes determined $\Delta R/R$ time evolution. Photoexcitation results in a rapid rise (~ 0.2 ps). It was followed by two distinct recovery processes. The initial rapid rise was due to carriers excitation. The rapid recovery process (τ_f) occurred within 0.3

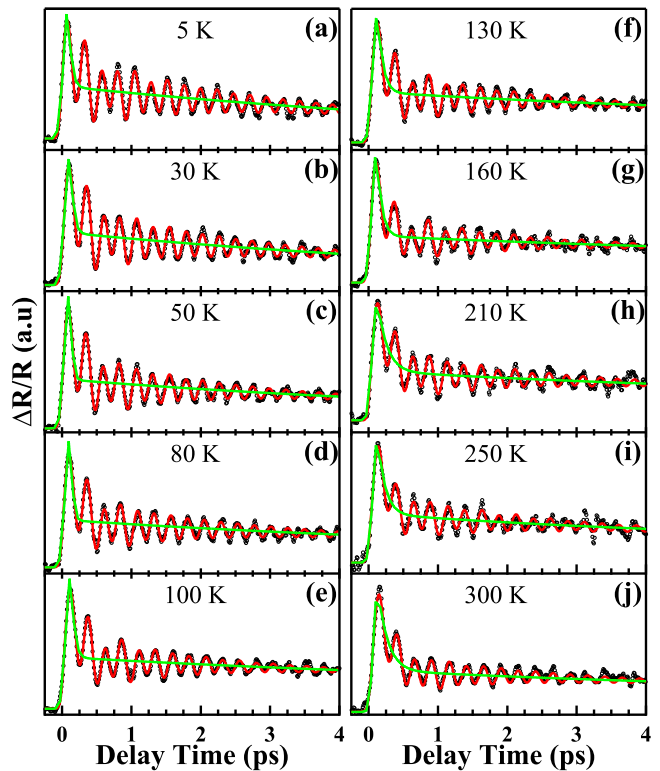


FIG. 2. (Color online) (a)-(j) $\Delta R/R$ PdTe₂ transient reflectivity in at several selected temperatures between 5 and 300 K. The solid red and green lines show fit to measured signal, with and without the oscillations, respectively.

ps. A slower relaxation (τ_s) then occurred. After an ~ 40 ps relaxation period, the signal was dominated by a flat offset which is indicated by a dashed blue line. Two significant high-frequency oscillations are superimposed on the $\Delta R/R$ profile. They are nearly simultaneous. This simultaneity is evidenced by the small asymmetric periodic wiggles in the Fig. 1. Relaxation curves are significantly affected by the large amplitudes of the two oscillations. The fast relaxation process τ_f lifetime is comparable to the pumping pulse duration. The signal de-convolved with a finite width Gaussian pump pulse. The solid red line in Fig. 1 suggests that the data fits well with

$$\frac{R(t)}{R} = \frac{1}{\sqrt{2\pi}w} \exp\left(-\frac{t^2}{2w^2}\right) \otimes \left[\sum_{i=1,2} A_i \exp\left(-\frac{t-t_0}{\tau_i}\right) + \sum_{j=1,2} B_j \exp(-\Gamma_j(t-t_0)) \sin(\Omega_j t + \phi_j) \right] + C$$

where A_i and τ_i are the amplitude, and relaxation times of the i th nonoscillatory signal, respectively, and describe carrier dynamics. B_j , Γ_j , Ω_j , and ϕ_j are j th oscillatory signal amplitude, damping rate, frequency, and initial phase, respectively. They describe the collective excitation dynamics. And w and C are incidence pulse temporal duration and a constant offset, respectively.

Fig. 2 displays $\Delta R/R$ differential reflectivity at se-

lected temperatures in the 5 K - 300 K range over a short time scale. The data are similar even at different temperatures. There are two distinct relaxation processes and two pronounced oscillations. Oscillations amplitude increased as temperature dropped. $\Delta R/R$ reflectivity fitted well with the formula at all measured temperatures.

First, we focus on the nonoscillatory response, i.e., the two relaxation processes. The quasiparticle dynamic quantitative analysis was studied for its temperature-dependent behavior and to gain insight into relaxation processes origins. The relaxation processes fitted well to the formula when oscillations were not included (set $B_j = 0$). Attracted decay times τ_f and τ_s were plotted as a function of temperature (Fig. 3). The rapid recovery process ($\tau_f < 0.2$ ps) slowed as the temperature drops. It saturated at ~ 100 K [Fig. 3(a)]. After femtosecond photoexcitation, electron temperatures rose, on a femtosecond time scale, to thousands of K. High-energy hot electrons then transferred excess energy to the lattice at a subpicosecond time scale through carrier-phonon interaction [37, 38]. The temperature dependence of τ_f was similar to that of the e - ph thermalization observed in other materials [32, 33, 39]. It seems reasonable to attribute τ_f in PdTe₂ to electronic system cooling via e - ph thermalization rather than the e - e scattering.

A two-temperature model (TTM) is usually used to describe temperature dependence of e - ph thermalization [32, 33, 39]. At low temperature, e - ph and e - e have comparable thermalization times. TTM is thus not a suitable model for low temperatures e - ph thermalization. PdTe₂ Θ_D is about 210 K [40]. According to the TTM mode used in previous literatures [32, 33, 39], we fitted the temperature dependent data above 80 K. Using optical properties measured by Heumen et al. [41], the laser energy density is determined to $U_l \simeq 1$ J/cm³. As shown by the dashed red line in Fig. 3(a), a very good fitting result is obtained, which supports the attributing τ_f to e - ph thermalization. Fitting τ_f data obtained an electronic specific heat coefficient $\gamma \simeq 4.3$ J·m⁻³K⁻², and an e - ph coupling constant $g_\infty \simeq 1.44 \times 10^{16}$ W·m⁻³K⁻¹.

According to the Allen's model of the thermal relaxation of electrons [37], the relaxation time τ of the quasiparticle in metals is given by

$$1/\tau = 3\hbar\lambda\langle\omega^2\rangle/\pi k_B T_e$$

where the λ is the e - ph coupling constant, $\lambda\langle\omega^2\rangle$ is the second momentum of Eliashberg function. T_e was derived from the TTM mode. From the measured relaxation time at 300 K, $\tau_f \sim 0.155$ ps, we obtained $\lambda\langle\omega^2\rangle \sim 6.6 \times 10^{26}$ Hz² = 285 meV². By use of $\langle\omega^2\rangle \sim 4.4 \times 10^4$ K² obtained from Debye model [40], we get $\lambda = 0.87$. The value of λ is larger than the result obtained by a recent theoretical study (0.57)[30] and transport measurement (0.59) [42]. The larger e - ph coupling constant λ indicates that PdTe₂ is an intermediately coupled superconductor,

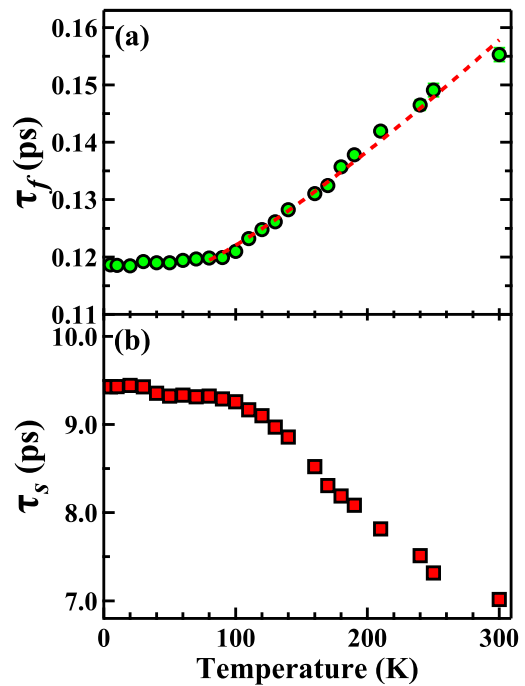


FIG. 3. (Color online) (a) shows τ_f and (b) shows τ_s , as a function of temperature. The dashed red curve denotes the TTM fit.

which will be important in understanding the BCS-type superconductivity in PdTe₂.

Fig. 3(b) illustrates slow component τ_s temperature dependence. Unlike τ_f , τ_s increased as temperature dropped until saturation at ~ 100 K. After the initial e - ph thermalization, excess electrons (holes) in the conduction (valence) bands would have moved closer to the Fermi energy (E_F). The τ_s origins can be revealed by examining Fermi Surface (FS) topologies and PdTe₂ band structure. Earlier ARPES measurements indicated that PdTe₂, like other semimetals [43, 44], coexists with electron and hole Fermi pockets [24–28, 36]. Naturally, τ_s originates from an e - h recombination between conduction and valence bands. This process exists widely in semimetals. The τ_s relaxation times are 7 ~ 10 ps and much faster than that of e - h radiative recombination which are a few nanoseconds [45]. Electron and hole Fermi pockets are separated in momentum space. Momentum conservation requires that e - h recombination processes be assisted by a third quasiparticle. It seems most likely that the phonon-assisted e - h recombination between electron and hole pockets is involved. This has been observed in other semi-metallics with similar temperature dependence behavior [32, 46].

Next, we analyze the dynamics of collective excitations in PdTe₂, which was superimposed on $\Delta R/R$ curves (Fig. 1 and Fig. 2). Optical phonon modes can be extracted by directly fitting the total dynamics trace with the function (Fig. 1 and Fig. 2, solid red lines), or by subtracting

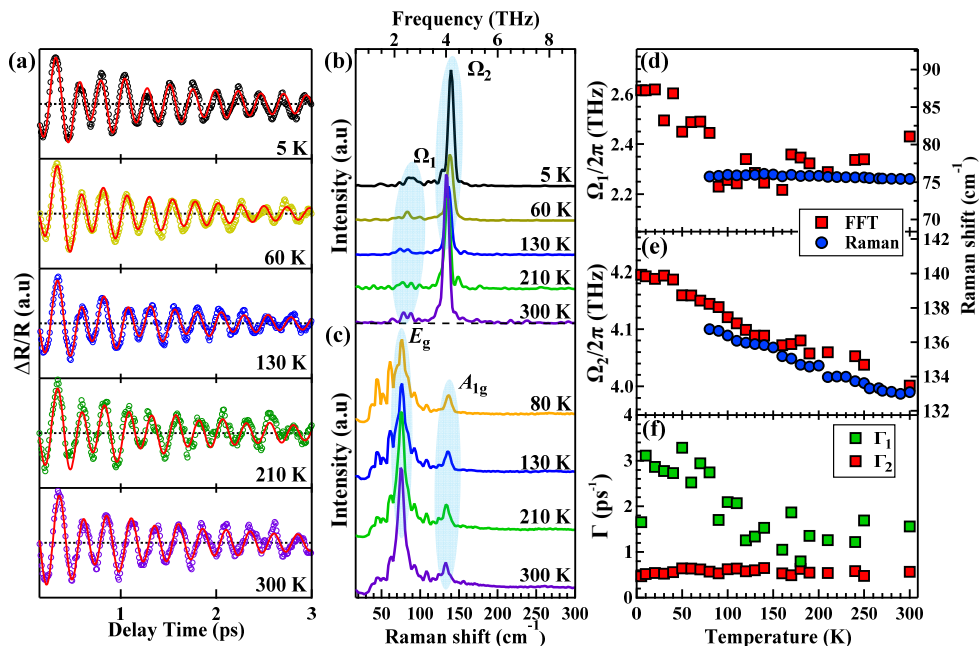


FIG. 4. (a) Extracted oscillations at noted temperatures. Fitted results are in red. (b) FFT frequency-domain data corresponding to (a). Curves are shifted vertically for legibility. (c) PdTe₂ Raman spectra at various temperatures. (d) and (e) show derived Ω_1 and Ω_2 as a function of temperature. The blue circles indicate the Raman shift of E_g and A_{1g} phonon modes. (f) The derived damping rate Γ_1 and Γ_2 of coherent optical phonon Ω_1 and Ω_2 , respectively.

the quasiparticle dynamics (Fig. 1 and Fig. 2, solid green lines) from the total-dynamics trace. This study used the latter approach. The time-domain oscillations for several selected temperatures were appeared in Fig. 4(a). The red curves are the fitting curves based on a two-components damped oscillation function. As usual, we use fast Fourier transform (FFT) to analyze the coherent collective excitations in the frequency domain. Two distinct high frequency terahertz modes (Ω_1) and (Ω_2) were resolved at all measured temperatures (Fig. 4). For the lower frequency Ω_1 mode, frequency domain data is relatively dispersed possibly due to intrinsically low phonon signal, but also because of that its cycle is about twice that of Ω_2 . During carriers relaxation processes, oscillations caused by collective excited states such as coherent phonons and charge density waves in the material are further manifested as reflectivity signal oscillations [47–49]. Usually, oscillatory components that persisting to room temperatures are attributed to coherent phonons. The phonons are initiated via dispersive excitations [50] or photoinduced Raman modes.

Raman scattering results are shown in Fig. 4(c). At least two significant vibrational modes were resolved. At room temperature (300 K), two Raman shift modes values are $\sim 75.4 \text{ cm}^{-1}$ and $\sim 133.2 \text{ cm}^{-1}$. These correspond, respectively, to Te atoms in-plane (E_g) and out-of-plane (A_{1g}) motions [46, 51, 52] respectively. These values are consistent with previous reports bulk PdTe₂ values [52]. Fig. 4(b) and (c) are plotted on

the same horizontal axis range. Frequencies of Ω_1 and Ω_2 are identical to that of E_g and A_{1g} phonons, respectively. This suggests that Ω_1 and Ω_2 originate from the E_g and A_{1g} phonons, respectively.

Ω_1 and Ω_2 frequencies were estimated by fitting the peak with a Gaussian lineshape. Fig. 4(d) and (e) display Ω_1 and Ω_2 frequencies derived from FFT, respectively, as a function of temperature. To compare with Raman scattering, E_g and A_{1g} Raman shift data were overlaid on FFT data in Fig. 4(d) and (e), respectively. At 5 K, Ω_1 and Ω_2 frequencies were about 2.6 and 4.2 THz, respectively. Ω_1 and Ω_2 , extracted by FFT, varied significantly with temperature. The Ω_2 (A_{1g}) mode frequency obtained from both ultrafast spectroscopy and Raman measurements revealed that it decreased monotonously as temperatures increased. When temperature increased from 5 to 300 K, Ω_2 mode redshifted about 0.2 THz. Instead of a monotonic Ω_1 decrease as temperature rose, it largely stabilized at temperatures above 80 K. By increasing the temperature from 5 K to 300 K, Ω_1 mode is redshifted even more dramatically. E_g measured by Raman scattering is almost constant at high temperatures. The extracted temperature dependence of damping rates Γ_1 , and Γ_2 , of Ω_1 and Ω_2 , respectively, are plotted in Fig. 4(f). The damping rate Γ_2 was almost constantly of $\sim 0.5 \text{ ps}^{-1}$ at all temperatures. Damping rate Γ_1 seemed to decrease as temperature increased and settled between $1 \sim 3.5 \text{ ps}^{-1}$.

In general, population decay along with pure dephas-

ing determined coherent phonons damping. Previous studies suggested that the coherent phonons decay processes in semimetal and topological insulators are largely determined by population decay caused by anharmonic phonon-phonon coupling [33, 46, 53, 54]. Phonon population is a strong function of temperature. Coherent phonon frequency and damping rates are strongly temperature-dependent. For anharmonic effects, usually, the frequency decreases as temperature rises while damping rate increases [33, 34, 46]. This is not the case with Ω_1 and Ω_2 modes. Coherent phonons, Γ_1 and Γ_2 , are not well explained in terms of anharmonic effects alone. Pure dephasing always exists because a quantum system is always connected to its surroundings. Previous studies have shown that PdTe₂ is a BCS-type superconductor. The above analysis indicates that PdTe₂ is an intermediately coupled superconductor. Pure dephasing, e.g., *e-ph* scattering, should accounted for.

III. IV. CONCLUSIONS

In this study, ultrafast time-resolved differential reflectivity and Raman scattering measurements were performed on PdTe₂ as a function of temperature to reveal important carriers and coherent phonons roles. Two exponential relaxation processes with distinctive time constants were readily observed. The origins of these two processes may be attributed to *e-ph* thermalization ($\tau_f < 0.2$ ps) and phonon-assisted *e-h* recombination ($\tau_s \sim 7$ -9.5 ps). Two vibrational modes were resolved as originating from Te atoms in-plane (E_g) and out-of-plane (A_{1g}) motions. Both E_g and A_{1g} phonon mode softens, resift, as temperatures rise from ~ 2.6 and 4.2 THz at 5 K to ~ 2.3 and 4.0 THz at 300 K, respectively. The *e-ph* scattering plays important roles in the relaxation process. Further careful studies are requested for to address the

ACKNOWLEDGMENTS

We are grateful for valuable discussions with J. Qi, C. C Shu, and M. X Chen. Our work was supported by the National Natural Science Foundation of China (Grants No. 12074436, and No. U2032204), and Chinese National Key Research and Development Program (2016YFA0300604). J. Q Meng would like to acknowledge support from the Innovation-driven Plan in Central South University (2016CXS032).

* Corresponding author: jqmeng@csu.edu.cn

[1] Y. I. Joe, X. M. Chen, P. Ghaemi, K. D. Finkelstein, G. A. de la Peña, Y. Gan, J. C. T. Lee, S. Yuan, J. Geck, G.

- J. MacDougall, T. C. Chiang, S. L. Cooper, E. Fradkin, and P. Abbamonte, Nat. Phys. **10**, 421 (2014).
- [2] P. Li, Y. Wen, X. He, Q. Zhang, C. Xia, Z. M. Yu, S. A. Yang, Z. Zhu, H. N. Alshareef, and X. X. Zhang, Nat. Commun. **8**, 2150 (2017).
- [3] H. Q. Huang, S. Y. Zhou, and W. H. Duan, Phys. Rev. B **94**, 121117(R) (2016).
- [4] P. Chen, W. W. Pai, Y. H. Chan, A. Takayama, C. Z. Xu, A. Karn, S. Hasegawa, M. Y. Chou, S. K. Mo, A. V. Fedorov, and T. C. Chiang, Nat. Commun. **8**, 516 (2017).
- [5] M. N. Ali, J. Xiong, S. Flynn, J. Tao, Q. D. Gibson, L. M. Schoop, T. Liang, N. Haldolaarachchige, M. Hirschberger, N. P. Ong, and R. J. Cava, Nature **514**, 205 (2014).
- [6] Xiao-Liang Qi, and Shou-Cheng Zhang, Rev. Mod. Phys. **83**, 1057 (2011).
- [7] M. Z. Hasan, and C. L. Kane, Rev. Mod. Phys. **82**, 3045 (2010).
- [8] M. Z. Hasan and S. Xu and G. Bian, Phys Scripta **T164**, 014001 (2015).
- [9] M. Sato and Y. Ando, Rep. Prog. Phys. **80**, 076501 (2017).
- [10] T. Das, and K. Dolui, Phys. Rev. B **91**, 094510 (2015).
- [11] K. Tsutsumi, Phys. Rev. B **26**, 5756 (1982).
- [12] P. K. Biswas, D. G. Mazzone, R. Sibille, E. Pomjakushina, K. Conder, H. Luetkens, C. Baines, J. L. Gavilano, M. Kenzelmann, A. Amato, and E. Morenzoni, Phys. Rev. B **93**, 220504(R) (2016).
- [13] H. Leng, C. Paulsen, Y. K. Huang, and A. de Visser, Phys. Rev. B **96**, 220506(R) (2017).
- [14] F. Fei, X. Bo, R. Wang, B. Wu, J. Jiang, D. Fu, M. Gao, H. Zheng, Y. Chen, X. Wang, H. Bu, F. Song, X. Wan, B. Wang, and G. Wang, Phys. Rev. B **96**, 041201(R) (2017).
- [15] Y. Hsu, A. Vaezi, M. H. Fischer, and E. Kim, Nat. Commun. **8**, 14985 (2017).
- [16] Y. T. Hsu, W. S. Cole, R. X. Zhang, and J. D. Sau, Phys. Rev. Lett. **125**, 097001 (2020).
- [17] J. Guggenheim and F. Hulliger and J. Müller, Helv. Phys. Acta **34**, 408 (1961).
- [18] Amit and Y. Singh, Phys. Rev. B **97**, 054515 (2018).
- [19] S. Teknowijoyo, N. H. Jo, M. S. Scheurer, M. A. Tanatar, K. Cho, S. L. Bud'Ko, P. P. Orth, P. C. Canfield, and R. Prozorov, Phys. Rev. B **98**, 024508 (2018).
- [20] J. A. Voerman, J. C. de Boer, T. Hashimoto, Y. Huang, C. Li, and A. Brinkman, Phys. Rev. B **99**, 014510 (2019).
- [21] H. Leng, J. C. Orain, A. Amato, Y. K. Huang, and A. de Visser, Phys. Rev. B **100**, 224501 (2019).
- [22] Tian Le, Lichang Yin, Zili Feng, Qi Huang, Liqiang Che, Jie Li, Youguo Shi, and Xin Lu, Phys. Rev. B **99**, 180504(R) (2019).
- [23] R. Chapai, D. A. Browne, D. E. Graf, J. F. DiTusa, and R. Jin, J. Phys. Condens. Matter **33**, 35601 (2020).
- [24] Y. Liu, J. Z. Zhao, L. Yu, C. T. Lin, A. J. Liang, C. Hu, Y. Ding, Y. Xu, S. L. He, L. Zhao, G. D. Liu, X. L. Dong, J. Zhang, C. T. Chen, Z. Y. Chen, H. M. Weng, X. Dai, Z. Fang, and X. J. Zhou, Chinese. Phys. L **32**, 067303 (2015).
- [25] H. J. Noh, J. Jeong, E. J. Cho, K. Kim, B. I. Min, and B. G. Park, Phys. Rev. Lett. **119**, 016401 (2017).
- [26] M. Z. Yan, H. Q. Huang, K. N. Zhang, E. Y. Wang, W. Yao, K. Deng, G. L. Wan, H. Y. Zhang, M. Arita, H. T. Yang, Z. Sun, H. Yao, Y. Wu, S. S. Fan, W. H. Duan, and S. Y. Zhou, Nat. Commun. **8**, 257 (2017).

- [27] M. S. Bahramy, O. J. Clark, B. J. Yang, J. Feng, L. Bawden, J. M. Riley, I. Marković, F. Mazzola, V. Sunko, D. Biswas, S. P. Cooil, M. Jorge, J. W. Wells, M. Leandersson, T. Balasubramanian, J. Fujii, I. Vobornik, J. E. Rault, T. K. Kim, M. Hoesch, K. Okawa, M. Asakawa, T. Sasagawa, T. Eknapakul, W. Meevasana, and P. D. C. King, *Nat. Mater.* **17**, 21 (2018).
- [28] O. J. Clark, M. J. Neat, K. Okawa, L. Bawden, I. Marković, F. Mazzola, J. Feng, V. Sunko, J. M. Riley, W. Meevasana, J. Fujii, I. Vobornik, T. K. Kim, M. Hoesch, T. Sasagawa, P. Wahl, M. S. Bahramy, and P. D. C. King, *Phys. Rev. Lett.* **120**, 156401 (2018).
- [29] T. R. Finlayson, W. Reichardt, and H. G. Smith, *Phys. Rev. B* **33**, 2473 (1986).
- [30] K. Kim, S. Kim, J. S. Kim, H. Kim, J. H. Park, and B. I. Min, *Phys. Rev. B* **97**, 165102 (2018).
- [31] J. Qi, T. Durakiewicz, S. A. Trugman, J. X. Zhu, P. S. Riseborough, R. Baumbach, E. D. Bauer, K. Gofryk, J. Q. Meng, J. J. Joyce, A. J. Taylor, and R. P. Prasankumar, *Phys. Rev. Lett* **111**, 057402 (2013).
- [32] Y. M. Dai, J. Bowlan, H. Li, H. Miao, S. F. Wu, W. D. Kong, P. Richard, Y. G. Shi, S. A. Trugman, J. X. Zhu, H. Ding, A. J. Taylor, D. A. Yarotski, and R. P. Prasankumar, *Phys. Rev. B* **92**, 161104(R) (2015).
- [33] L. Cheng, C. La-o-vorakiat, C. S. Tang, S. K. Nair, B. Xia, L. Wang, J. Zhu, and E. E. M. Chia, *Appl. Phys. Lett* **104**, 211906 (2014).
- [34] Y. P. Liu, Y. J. Zhang, J. J. Dong, H. Lee, Z. X. Wei, W. L. Zhang, C. Y. Chen, H. Q. Yuan, Y. F. Yang, and J. Qi, *Phys. Rev. Lett* **124**, 057404 (2020).
- [35] S. Z. Zhao, H. Y. Song, L. L. Hu, T. Xie, C. Liu, H. Q. Luo, C. Y. Jiang, X. Zhang, X. C. Nie, J. Q. Meng, Y. X. Duan, S. B. Liu, H. Y. Xie, and H. Y. Liu, *Phys. Rev. B* **102**, 144519 (2020).
- [36] Y. Liu, J. Z. Zhao, L. Yu, C. Lin, C. Hu, D. Liu, Y. Peng, Z. Xie, J. He, C. Chen, Y. Feng, H. Yi, X. Liu, L. Zhao, S. He, G. Liu, X. Dong, J. Zhang, C. Chen, Z. Xu, H. Weng, X. Dai, Z. Fang, and X. J. Zhou, *Chinese Phys B* **24**, 067401 (2015).
- [37] P. B. Allen, *Phys. Rev. Lett* **59**, 1460 (1987).
- [38] R. H. M. Groeneveld and R. Sprik and A. Lagendijk, *Phys. Rev. B* **51**, 11433 (1995).
- [39] J. Demsar, R. D. Averitt, K. H. Ahn, M. J. Graf, S. A. Trugman, V. V. Kabanov, J. L. Sarrao, and A. J. Taylor, *Phys. Rev. Lett* **91**, 027401 (2003).
- [40] K. Kudo, H. Ishii, and M. Nohara, *Phys. Rev. B* **93**, 140505(R) (2016).
- [41] J. A. Voerman, J. C. de Boer, T. Hashimoto, Yingkai Huang, Chuan Li, and A. Brinkman, *Phys. Rev. B* **99**, 014510(2019).
- [42] M. K. Hooda, and C. S. Yadav, *EPL* **121**, 17001(2018).
- [43] J. Jiang, F. Tang, X. C. Pan, H. M. Liu, X. H. Niu, Y. X. Wang, D. F. Xu, H. F. Yang, B. P. Xie, F. Q. Song, P. Dudin, T. K. Kim, M. Hoesch, P. K. Das, I. Vobornik, X. G. Wan, and D. L. Feng, *Phys. Rev. Lett.* **115**, 166601 (2015).
- [44] X. F. Tang, Y. X. Duan, F. Y. Wu, S. Y. Liu, C. Zhang, Y. Z. Zhao, J. J. Song, Y. Luo, Q. Y. Wu, J. He, H. Y. Liu, W. Xu, and J. Q. Meng, *Phys. Rev. B* **99**, 125112 (2019).
- [45] A. Othonos, *J. Appl. Phys.* **83**, 1789 (1998).
- [46] S. X. Zhu, C. Zhang, Q. Y. Wu, X. F. Tang, H. Liu, Z. T. Liu, Y. Luo, J. J. Song, F. Y. Wu, Y. Z. Zhao, S. Y. Liu, T. Le, X. Lu, H. Ma, K. H. Liu, Y. H. Yuan, H. Huang, J. He, H. Y. Liu, Y. X. Duan, and J. Q. Meng, *arXiv:2012.01645V1* (2020).
- [47] K. S. Burch, E. E. M. Chia, D. Talbayev, B. C. Sales, D. Mandrus, A. J. Taylor, and R. D. Averitt, *Phys. Rev. Lett* **100**, 026409 (2008).
- [48] A. Tomeljak, H. Schäfer, D. Städter, M. Beyer, K. Biljakovic, and J. Demsar, *Phys. Rev. Lett* **102**, 066404 (2009).
- [49] R. Y. Chen, S. J. Zhang, M. Y. Zhang, T. Dong, and N. L. Wang, *Phys. Rev. Lett* **118**, 107402 (2017).
- [50] H. J. Zeiger, J. Vidal, T. K. Cheng, E. P. Ippen, G. Dresselhaus, and M. S. Dresselhaus, *Phys. Rev. B* **45**, 768 (1992).
- [51] A. Vymazalov, F. Zaccarini, and R. J. Bakker, *Eur J Mineral* **26**, 711 (2014).
- [52] E. Li, R. Z. Zhang, H. Li, C. Liu, G. Li, J. O. Wang, T. Qian, Y. Y. Zhang, S. X. Du, X. Lin, and H. J. Gao, *Chinese Phys. B* **27**, 086804 (2018).
- [53] M. Balkanski and R. F. Wallis and E. Haro, *Phys. Rev. B* **28**, 1928 (1983).
- [54] J. Menéndez and M. Cardona, *Phys. Rev. B* **29**, 2051 (1984).